

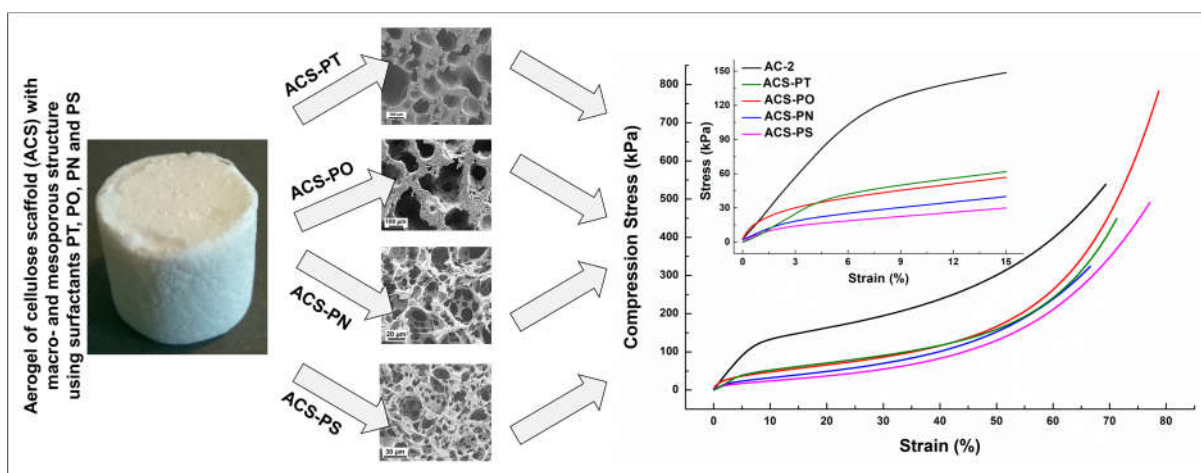
# INFLUENCE OF HIERARCHICAL POROUS STRUCTURES ON THE MECHANICAL PROPERTIES OF CELLULOSE AEROGELS

Kathirvel Ganesan\*, Adam Barowski, Lorenz Ratke, Barbara Milow

Institute of Materials Research, German Aerospace Center, Linder Hoehe, 51170 Cologne, Germany.

Corresponding author email address: k.ganesan@dlr.de

## Graphical abstract



# INFLUENCE OF HIERARCHICAL POROUS STRUCTURES ON THE MECHANICAL PROPERTIES OF CELLULOSE AEROGELS

Kathirvel Ganesan\*, Adam Barowski, Lorenz Ratke, Barbara Milow

Institute of Materials Research, German Aerospace Center, Linder Hoehe, 51170 Cologne, Germany

Corresponding author email address: k.ganesan@dlr.de

**Abstract:** Aerogels of cellulose exhibit remarkable mechanical properties as a function of density. Modifying the pore volume in classical cellulose aerogels using sacrificial template methods provide scaffold like microstructure. In the present study, we have developed aerogels of cellulose scaffolds having almost same density values but differ in microstructure and analysed the influence on the mechanical properties of bulk materials. This study can give an insight into the materials design for advanced engineering materials. Employing four surfactants having difference in hydrophilic-lipophilic balance (HLB), namely polyoxyethylene *tert*-octylphenyl ether (PT), polyoxyethylene (20) oleyl ether (PO), polyoxyethylene (40) nonylphenyl ether (PN) and polyoxyethylene (100) stearyl ether (PS), the cellulose scaffolds with hierarchical porous structures were developed. The mechanical properties of cellulose scaffolds were compared with classical pure cellulose aerogels. The results indicate that the solid fraction of cellulose nanofibers per unit volume of cell walls of scaffolds plays an important role in determining the elastic properties and strength. As the nanofibrils support the cell walls of scaffolds, Young's modulus can be improved if the concentration of cellulose nanofibers is high at the cell walls or cell wall thickness is larger. The scaffold materials of this kind could be used as supporting materials with desired properties for filter, catalysis and biomedicine.

**Keywords:** Cellulose; Aerogel; Scaffolds; Hierarchical structure; Porous network.

## Highlights:

- The aerogels of cellulose scaffolds with hierarchical porous structures were developed.
- The hierarchical porous structures were designed by using four different surfactants.
- The entrapped oil droplets in the cellulose matrix act as a structural template.
- The solid fraction per unit volume of cell walls of scaffolds influences the mechanical property.
- The structural design of pore channels play major role in defining the elastic property.

## 1 Introduction

Aerogels of cellulose are one of the classes of open porous lightweight materials. They possess interconnected nanofibrillar network with high specific surface area. The production of regenerated cellulose aerogels is widely developed by physical dissolution and regeneration of cellulose from different solvent media [1,2]. Regenerated cellulose aerogels exhibit poor crystallinity, most often cellulose II [3-5], though the only exception was recently reported when zinc chloride tetrahydrate was used as a solvent [6]. The pore size distribution was polydisperse, ranging from mesopores to few hundred nanometers of macropores. Depending upon the concentration of cellulose content, the pore size distribution varies, that means the envelope density exhibits a linear relationship with cellulose concentration [7-10,2]. As a function of density, the bulk materials have improved mechanical properties [6,7].

Bringing in the hierarchical porous structures in cellulose-based materials can provide the lightweight skeleton and pore volume with the desired mechanical function, mass transport and storage and/or adsorption properties.

Designing the cellulose porous structures with a lot of useful properties is a rapidly growing field of interests [11-15] due to the fact that cellulose is a non-toxic, biodegradable and environmentally friendly polymer. Sacrificial template methods can be employed for engineering the porous structures [13-16] where frozen ice, porogen particles or surfactant-stabilized oil droplets act as structural template producing macropores replicating the shape of the templates. The modification of size and shape of the templates can yield diversified porous structures. In many literatures, frozen ice crystal-template was mostly employed to produce macroporous structures by controlling freezing conditions during freeze drying of the wet gels [11,15,16]. Pircher et al. have produced hierarchical porous structures using porogen-type particles as templates and employing supercritical CO<sub>2</sub> drying [13]. In our recent publication, we have employed oil-droplets as template to produce hierarchical porous structures in which the diversified physical properties were developed by utilizing different drying

techniques, namely supercritical CO<sub>2</sub> drying, freeze drying and ambient drying. In all the reported literatures, the bulk density and porosity of cellulose aerogels had direct influence on the mechanical properties.

In the present paper, we demonstrate the influence of hierarchical porous structures on the mechanical properties of cellulose aerogels having almost the same values of relative density and same porosity. The understandings from these studies can provide insight into the materials design for advanced engineering materials. For that we have adapted the surfactant-stabilized oil template method to produce the hierarchical porous structures using surfactants having different hydrophilic-lipophilic balance (HLB). The following surfactants have been chosen: polyoxyethylene *tert*-octylphenyl ether (PT; HLB = 13.5), polyoxyethylene (20) oleyl ether (PO; HLB = 15), polyoxyethylene (40) nonylphenyl ether (PN; HLB = 17) and polyoxyethylene (100) stearyl ether (PS; HLB = 18) in order to modify the hierarchical porous structures. Employing these surfactants, the cellulose aerogels having same physical properties have been prepared, but huge differences in microstructures composing hierarchical porous structures have been observed. The distribution of meso- and macroporous structures in the cellulose matrix and the supporting nanofibrils in the cell walls of cellulose scaffolds play a significant role in influencing the mechanical properties. The cellulose aerogel materials produced by this method with desired physical and structural properties could be utilized as supporting materials with desired properties for applications such as filter, catalysis and biomedicine.

## **2 Experimental**

### **2.1 Materials and methods**

All chemicals were used as received. Microcrystalline cellulose (medium fibres, product number is C6288), calcium thiocyanate tetrahydrate (95%), glyceryl trioctanoate, polyoxyethylene *tert*-octylphenyl ether (Triton<sup>TM</sup> X-100; PT), polyoxyethylene (20) oleyl ether (Brij<sup>®</sup> 98; PO), polyoxyethylene (40) nonylphenyl ether, branched (IGEPAL<sup>®</sup> CO-890; PN) and polyoxyethylene (100) stearyl ether (Brij<sup>®</sup> S 100; PS) were purchased from Sigma-Aldrich. Hydrophilic-lipophilic balance values of surfactants were obtained from the materials safety data sheet. In the gel preparation process deionized water was used. Supercritical drying was carried out in an autoclave using pure carbon dioxide, following the procedure reported by Hoepfner et al [8]. The products were characterized by envelope density measurement (Micromeritics - GeoPyc 1360), skeletal density (Micromeritics - Accupyc II 1340; Gas pycnometer - Helium), BET nitrogen adsorption-desorption isotherm analysis (Micromeritics - Tristar II 3020). The skeletal density was observed to be 1533 g/l, after analysing various

samples of cellulose. Compression tests were performed on a universal testing machine from Latzke using samples of cylindrical shape (~10 mm diameter and ~10 mm height) and a compression rate of 1 mm/min. For soft samples a force head with 100 N and for hard samples a force head of 500 N were used. The mechanical data presented below in the results section are averages of at least three measurements and the standard deviation is given, showing that the reproducibility is around 1-3 %. The physical properties and the mechanical data of AC-4 and ACS-PO were newly collected for freshly prepared samples and characterized although they were previously reported in literature [14]. The data of AC-2 were adapted from the previous report [14]. The relative density of the cellulose materials is calculated from the ratio between envelope density ( $\rho_e$ ) and skeletal density ( $\rho_s$ ). However the traces of removal of calcium thiocyanate and the cleanliness of cellulose aerogels were confirmed as per the methods reported in our earlier literature [14]. The crystallinity of aerogel materials was confirmed to be cellulose II [14]. The microstructure was analysed on the SEM pictures using the ImageJ program by first thresholding the images to reveal the macropores and the cell walls. Then 10 -15 equidistant lines were superimposed over the resulting binary image and the linear intercept in the macropores determined, in the cell walls and the macroporosity was determined from the ratio of the line length in the pores in relation to the total line length on the image. In addition the macroporosity was determined on the binary images by directly evaluating the number of pixels in the macropores and relating it to the total number of pixels in the image.

## 2.2 Synthesis of cellulose aerogels

The aerogels and aerogel scaffolds were prepared by the methods reported in literature [14]. Classical aerogels of cellulose containing 2 and 4 wt% of cellulose were abbreviated in the text as AC-2 and AC-4. Aerogels of cellulose scaffolds (ACS) prepared using four different surfactants, PT, PO, PN and PS which were labelled as ACS-PT, ACS-PO, ACS-PN and ACS-PS respectively. Cellulose (4 wt%) and calcium thiocyanate tetrahydrate (96 g) were mixed together in the presence of water (80 mL) and heated up to 117 °C. Once the dissolution of cellulose was confirmed, the hot (125 °C) oil and surfactant mixture was added to it. After 15 minutes stirring at 150 rpm, the mixture was transferred to the mould and cooled to room temperature. After 16 hours, the gel body was washed first with acetone and then several times with ethanol. The alcogels were dried under supercritical condition to get aerogels of cellulose scaffolds.

Although the oil and surfactant mixture were prepared by the same way how it was reported [14], the properties of surfactants should be taken into account. PT is a clear liquid and can be easily miscible in the oil phase. Other

surfactants were waxy solids having melting points close to room temperature. PS has highest melting point that is 51-54 °C in comparison with PN (46-47 °C) and PO (30-40 °C). Therefore the waxy solid was dispersed in the oil phase and the surfactants were molten above the melting point and homogeneously dispersed in the oil phase. Understanding the HLB values, PS with its long polyoxyethylene chain (HLB = 18) is more hydrophilic than PN (HLB = 17), PO (HLB = 15) and PT (HLB = 13.5). Adapting the synthesis procedure reported in literature [14], changing the surfactants from PO to PT, PN and PS unaffected the entrapment of oil droplets and the cellulose gel appearance had no difference.

### **3 Results and discussion**

#### **3.1 Synthesis of cellulose aerogels**

We have adapted the surfactant-stabilized oil template method for designing the cellulose aerogels having hierarchical porous structures. Figure 1 shows the schematic diagram of the synthesis method preparing the cellulose scaffolds. In this method, after mixing oil and surfactant mixture to the cellulose solution, oil droplets were entrapped into the cellulose-dissolved molten calcium thiocyanate hydrate during gelation. The surfactants PT, PO, PN and PS play an important role in stabilizing the oil droplets entrapped in cellulose solution during gelation by controlling the surface tension between the immiscible liquids, cellulose solution and oil. In this method of scaffolds preparation, the surfactant stabilized oil droplets act as a structural template. There was no difficulty in removing oil droplets and surfactant from the cellulose matrix. They were easily washed out together with calcium thiocyanate tetrahydrate by alcohol. After washing and supercritical drying, the hierarchical porous structures were established in the cellulose aerogel matrix.

#### **3.2 Physical properties of cellulose aerogels**

The physical properties of cellulose scaffolds are summarized in Table 1. After supercritical drying, apparently, the aerogels had volume shrinkage from the alcogels. It was observed to be 8.5 % for AC-4 and ranging 16 to 21 % for AC-2, ACS-PT, ACS-PO, ACS-PN and ACS-PS. ACS had very similar values of envelope density in comparison with AC-2. In the cellulose scaffolds preparation, the concentration of cellulose content is 4 wt%. The addition of equivalent weight percentage of oil caused bringing in additional macropore volume and simultaneously it reduced the density of the final cellulose material. The envelope density of cellulose aerogels with 4wt %, AC-4 was 115 g/L. After bringing in the hierarchical macropore structure, the envelope density

value of cellulose scaffolds was around 55 g/L. But the porosity got improved (see Table 1). It was almost same value for AC-2 and ACS being in average about 96 %.

The BET isotherm linear plot of ACS-PT is shown in supplementary information (Fig. SI-1). It showed the type IV isotherm according IUPAC nomenclature. There was no major difference between the BET specific surface area values of ACS-PT, ACS-PO and AC-2 which was in the range between 287 and 303 m<sup>2</sup>/g whereas the scaffolds ACS-PN and ACS-PS showed lower value (262 and 245 m<sup>2</sup>/g respectively). It can be reasoned out that due to the high hydrophilicity of PS (HLB = 18) and PN (HLB = 17), the surfactant could have good physical interactions with cellulose chains through the hydrogen bonding in comparison with the surfactant, PT and PO. During gelation and washing process, the surfactants may have influenced the assembly of cellulose chains during formation of nanofibers.

### 3.3 Microstructures of cellulose aerogels

In Figure 2, the scanning electron microscopy images of classical cellulose aerogel samples are compared. The image of AC-2 and AC-4 show finely distributed nanofibrillar structure with meso- and macropores. It is clearly observed that the macropore sizes are in the range between 100 nm and 1 μm. The magnified images on the right side show the nanofiber thickness that was estimated to be in the range between 8 and 12 nm.

Figure 3, 4, 5 and 6 show the microstructures of aerogel scaffolds, ACS-PT, ACS-PO, ACS-PN and ACS-PS respectively. The images showed the distribution of macropores which were produced by oil template method and the dimensions of the cell walls. The interesting features in the cell walls of scaffolds were the interconnected nanofibrillar structures (Fig. 3d and 4b) and the finely distributed secondary porous structures (2 to 200 nm). The nano-felt fibre thickness was about 8-12 nm.

In the case of ACS-PT, the scaffolds with a very wide distribution of macropore sizes, 50 to 600 μm were observed (Fig. 3a). The microstructure seemed to be closed foam structure if the pores (Fig. 3d) in the cell walls were not taken into consideration. The macropores produced by oil templates were observed to be close to spherical shape and they were interconnected through pores on the cell walls. There, only few neck parts were noticed between the macropores (Fig. 3c) which were about 10 to 20 μm in size. These neck parts of macropores could have been produced due to the coalescence of oil droplets during gelation. Mostly, the cell wall thickness varied between 750 nm and 1 μm. In some parts, the node point with thicker cell walls (30 – 100 μm) between 3 and 5 cells were observed.

In the case of ACS-PO, the macropores size distribution was ranging from 100 to 400  $\mu\text{m}$  and the size and shapes of pore channels vary (Fig. 4a). The cell wall thickness was in the range between 35 to 175  $\mu\text{m}$ . As it can be seen, no circular or spherical shapes were found and the macropore shapes were seemed to be an interconnected worm-like structure. The neck parts of the macropores were noticed to be in the size range 50 to 100  $\mu\text{m}$ .

In the case of ACS-PN and ACS-PS, the macropores were smaller in size. ACS-PN showed also wide range of macropores and they were close to spherical in shape (Fig. 5). It was noticed that a macropore (30-40  $\mu\text{m}$ ) possessed many neck parts (4-20  $\mu\text{m}$ ). The cell wall thickness was about 1-3  $\mu\text{m}$ .

For ACS-PS, the macropore size distribution was in the range between 2 and 35  $\mu\text{m}$  (Fig. 6). The shapes of macropores were almost close to spherical. As it can be observed, the bigger macropores (20-30  $\mu\text{m}$ ) were interconnected to each other with many neck parts with a size range of about 2-10  $\mu\text{m}$ . The cell wall thickness was about 250 nm-2  $\mu\text{m}$ .

These huge morphological differences in the cellulose scaffolds are accomplished by using the surfactants with different HLB values. It can be concluded from SEM data that increasing the HLB value of surfactant (PS; HLB = 18) can stabilize smaller oil droplets resulting in producing macropores being about 80% smaller in size and reducing the cell wall thickness maximum about 96-98 %.

### **3.4 Mechanical properties of cellulose aerogels**

The mechanical properties of the cellulose materials are compared in Table 2. The solid fraction of cellulose, i.e., relative density of the materials did not show major difference because of their nearly same physical properties like volume shrinkage, envelope density and porosity. Figure 7 shows the compression stress-strain curve of the cellulose materials. In the deformation process during compression, the stress-strain curve of cellulose materials show initially a rapid increasing elastic regime, after then smooth plastic collapse region and finally densification after 65 % of strain. The compressive strength of the material is taken from the yield stress at 1 % of strain (see table 2). Bringing hierarchical structures to the aerogel of cellulose 4 wt%, AC-4, not only decreased the envelope density about 50 %, but also caused severe impact on the mechanical properties by drastically decreasing the elastic modulus and yield strength. In general decreasing the relative density of the open porous materials decreases the Young's modulus, lowers the yield stress and decreases the energy adsorbed per unit volume.

In the present study the chosen materials, AC-2, ACS-PT, ACS-PO, ACS-PN and ACS-PS have nearly close values of relative density, i.e., the solid fraction in the bulk material is almost near constant values. Comparing with the AC-2, ACS samples had lower yield stress, about 3 to 6 times lesser than AC-2. As the initial linear elasticity is caused by the bending of the nanofibrils in the open pore space, the elastic modulus of aerogels and aerogel scaffolds are relying on how the nanofibrils are distributed in the matrix. For the comparison of ACS materials, the neck diameters, the distribution of macropore sizes and cell wall thickness should be taken into consideration.

For the comparison of structural and mechanical properties of classical aerogels of cellulose and cellulose scaffolds, first the aerogels of AC-2 and ACS-PO should be discussed as the structural differences shows great impact on Young's modulus data. In the case of AC-2, the elastic deformation occurs by simply folding up the nanofibrils continuously throughout the sample preceding the plastic deformation. Comparing the elastic modulus with AC-2, the samples ACS-PO acquire a slightly higher elastic modulus. This suggests that the nanofibrils in the cell walls of scaffold, ACS-PO preferably undergo elastic deformation followed by elastic deformation of the cell walls. Further, due to the bigger macropores and thicker cell walls, the cell wall bending can contribute to the elastic modulus. In order to follow the microstructural changes in plastic region, the compression test experiment was carried out on ACS-PO sample up to 25 % strain and the scanning electron microscopic images were taken before and after the measurements (see Fig. 8a and 8b). Figure 8b represents the deformation of cell walls during plastic collapse at 25% of strain which are bending, plastic collapse and buckling of the cell walls. The interconnected pore structures perpendicular to the compression axis are immediately forced to undergo cell wall collapse in comparison with the pores aligned in the parallel direction. And it suggests that the thicker cell walls with interconnected nanofibrillar supports resist the loading of compression stress whereas thinner cell walls fail.

The elastic modulus of ACS-PS with thin cell walls (250 nm-2  $\mu$ m) had a lowest Young's modulus of 0.63 MPa. In comparison with AC-2 and ACS-PO, due to the less solid fraction of cellulose and the closely packed smaller macropores (3-30 $\mu$ m), the nanofibrils in the cell walls of ACS-PS fail to bear the compressive stress. In comparison with ACS-PS, ACS-PN shows little higher Young's modulus and lower yield stress. Both of these samples have macropore size in average diameter about 30  $\mu$ m and many holes on their cell walls, i.e. neck parts between two cell walls. In this case, the neck diameter between two macropores should be taken into account. The neck diameter of ACS-PS is about two times smaller than ACS-PN. The smaller pore size provides more with standing strength than the bigger pores. Therefore, ACS-PN with its bigger macropore and neck diameter

results in high Young's modulus and low yield stress in comparison with the ACS-PS. However the failure of mechanical resistance of ACS-PS proposes that the nanofibrils in the cell walls undergo elastic deformation and then plastic collapse occurs by simply folding up the cell walls.

In the case of ACS-PT, due to the random arrangement of macropores with a wide range of pore size, thin and thick cell walls and very less cellular packing with neck parts (maximum neck size about 20  $\mu\text{m}$ ), the cellular scaffold material loses its elastic property. Young's modulus of ACS-PT is 2.4 times lesser than ACS-PO. On the contrary, yield stress of ACS-PT is little higher than ACS-PO. Here, the major stress resistance property comes from cellular packing with no neck parts. That means the nanofibrils present in the cell walls provide good impact on yield stress.

From the SEM pictures of ACS-PT one can show by image analysis that the volume of the macro pores is around 55% and the cell walls partly have a thickness of around 120  $\mu\text{m}$ . The material ACS-PT has almost spherical pores with thinner cell walls than ACS-PO. Image analysis of ACS-PO reveals a macro pore volume of 58% and a cell wall thickness in the range 35-175  $\mu\text{m}$ . It also looks as if the cell walls have only a few holes connecting them to other pores. ACS-PN has very thin cell walls with many holes in them. The macro pore volume is around 71 % and the cell walls have a thickness of only 2  $\mu\text{m}$ . ACS-PS has also very thin cell walls, around 2  $\mu\text{m}$  thick, but much they have more holes in them in comparison with ACS-PN. The macro pore volume fraction is estimated to be 72 %. The relative density of all materials is, however, almost constant at 0.04 despite the large difference in observable macro pore volume. This must mean that the solid fraction of cellulose inside the cell walls is different. Addition to that point, BET specific surface area of ACS-PS indicates that the fibril thickness of cellulose may be bigger than other ACS samples. One can make a simple calculation as follows. If  $\varphi_{cw}$  denotes the solid fraction inside the cell walls,  $\rho_{cw}$  the envelope density of the cell walls, then the envelope density of the macro-meso porous materials is simply given by  $\rho_e = \varphi_{cw} \rho_{cw}$  where we have neglected the term stemming from the density of air inside the pores. The envelope density of the pore walls is, however related to the solid fraction of cellulose  $\varphi_s$  inside them, meaning  $\rho_{cw} = \varphi_s \rho_s$ . Thus we have that the relative density is  $\rho_{rel} = \rho_e / \rho_s = \varphi_{cw} \varphi_s$ . The small variation in relative density of the four materials includes a larger variation of solid cellulose fraction in the cell walls. One can calculate a variation between 8% for ACS-PO and 13% for ACS PS and -PN. This means, the cellulose fibrils in the cell walls of ACS-PS and -PN are closer packed or thicker fibrils.

In porous body theory [17] Young's modulus of open or closed cell foams depends essentially to some power on the relative density. Since this value has only a small variation in the macro-meso porous material, the scaling

laws derived by Gibson and Ashby fail. This is especially clear looking at the yield strength at 1% plastic strain. The values of the four materials differ by a factor of 3, but there is no trend with either the relative density or the macropore volume or the cell wall thickness.

Nevertheless, summarizing the results, the elastic behaviour reflects the microstructure: ACS-PS and -PN have the thinnest cell walls with many holes in them and therefore they should have a low elastic modulus. ACS-PT has the anisotropic cell structure with less neck parts between two cells and lowest volume fraction of macropore and therefore, its Young's modulus should be larger than ACS-PS and ACS-PN. Especially ACS-PO with the thickest cell walls should have the highest Young's modulus. The stress needed to plastically deform ACS-PS and -PN should be smaller than that of the other two, since first they have large pores into which any deformation or buckling of the walls can easily be extended without touch neighbouring walls and secondly their cell walls are rather thin and can buckle easily.

Although thus qualitatively one can understand the mechanical behaviour we are currently of from a mathematical model to describe the deformation curves of this new material.

#### **4 Conclusion**

We have demonstrated the influence of hierarchical porous structures on the mechanical properties of cellulose aerogels by designing scaffold materials using two surfactants, PO and PS. In the case of ACS-PO, randomly arranged worm-like macropores (maximum 250  $\mu\text{m}$  width) were observed whereas in the case of ACS-PS smaller macropores (maximum about 30  $\mu\text{m}$ ) were found. The results indicate that combining the hierarchical structures with macropore size above 100  $\mu\text{m}$ , the cell wall thickness above 50  $\mu\text{m}$  and the nanofibrillar network in the cell walls, it can be possible to enhance the elastic property of the scaffolds materials, which can be comparable to pure aerogels of cellulose having similar relative density values. The solid fraction of cellulose nanofibers per unit volume of the cell walls is an absolutely essential criteria to enhance the mechanical properties. As the interconnected nanofibrillar structure in scaffolds structures supports the cell walls, the bulk hierarchical porous structure is resisting the compression to some extent until the elastic deformation of nanofibrils fails. This new method of scaffolds preparation can be generalized to tune the hierarchical structures in micro- and macroscopic dimensions using different surfactants. These pure scaffold materials of cellulose with hierarchical structures could be used as supporting materials in variety of applications like filters, catalysis and biomedicine.

## **References**

1. Wang S, Lu A, Zhang L (2016) Recent advances in regenerated cellulose materials. *Prog Polym Sci* 53:169-206
2. Ratke L (2011) Monoliths and fibrous cellulose aerogels. In: Aegerter MA, Leventis N, Koebel MM (eds) *Aerogels Handbook. Advances in Sol-Gel Derived Materials and Technologies*. Springer, New York, p 173
3. Budtova T, Navard P (2016) Cellulose in NaOH-water based solvents: a review. *Cellulose* 23:5-55
4. Cai J, Kimura S, Wada M, Kuga S, Zhang L (2008) Cellulose Aerogels from Aqueous Alkali Hydroxide–Urea Solution. *ChemSusChem* 1:149-154
5. Wan C, Lu Y, Jiao Y, Cao J, Sun Q, Li J (2015) Cellulose aerogels from cellulose–NaOH/PEG solution and comparison with different cellulose contents. *Mater Sci Technol* 31 (9):1096-1102
6. Rege A, Schestakow M, Karadagli I, Ratke L, Itskov M (2016) Micro-mechanical modelling of cellulose aerogels from molten salt hydrates. *Soft Matter* 12:7079-7088
7. Schestakow M, Karadagli I, Ratke L (2016) Cellulose aerogels prepared from an aqueous zinc chloride salhydrate melt. *Carbohydr Polym* 137:642-649
8. Hoepfner S, Ratke L, Milow B (2008) Synthesis and characterisation of nanofibrillar cellulose aerogels. *Cellulose* 15:121-129
9. Jin H, Nishiyama Y, Wada M, Kuga S (2004) Nanofibrillar cellulose aerogels. *Colloids and Surfaces A: Physicochem Eng Aspects* 240:63-67
10. Buchtová N, Budtova T (2016) Cellulose aero-, cryo- and xerogels: towards understanding of morphology control. *Cellulose* 23 (4):2585-2595
11. Pääkkö M, Vapaavuori J, Silvennoinen R, Kosonen H, Ankerfors M, Lindström T, Berglund LA, Ikkala O (2008) Long and entangled native cellulose I nanofibers allow flexible aerogels and hierarchically porous templates for functionalities. *Soft Matter* 4:2492-2499
12. Li VC-F, Dunn CK, Zhang Z, Deng Y, Qi HJ (2017) Direct Ink Write (DIW) 3D Printed Cellulose Nanocrystal Aerogel Structures. *Sci Rep* 7 (1):8018
13. Pircher N, Fischhuber D, Carbajal L, Strau C, Nedelec J-M, Kasper C, Rosenau T, Liebner F (2015) Preparation and Reinforcement of Dual-Porous Biocompatible Cellulose Scaffolds for Tissue Engineering. *Macromol Mater Eng* 300:911-924
14. Ganesan K, Dennstedt A, Barowski A, Ratke L (2016) Design of aerogels, cryogels and xerogels of cellulose with hierarchical porous structures. *Mater Des* 92:345-355
15. Deng M, Zhou Q, Du A, van Kasteren J, Wang Y (2009) Preparation of nanoporous cellulose foams from cellulose-ionic liquid solutions. *Mater Lett* 63 (21):1851-1854
16. Svagan AJ, Jensen P, Dvinskikh SV, Furó I, Berglund LA (2010) Towards tailored hierarchical structures in cellulose nanocomposite biofoams prepared by freezing/freeze-drying. *J Mater Chem* 20:6646-6654
17. Gibson LJ, Ashby MF (1997) *Cellular solids: structure and properties*. Second edn. Cambridge University Press, United Kingdom

# INFLUENCE OF HIERARCHICAL POROUS STRUCTURES ON THE MECHANICAL PROPERTIES OF CELLULOSE AEROGELS

Kathirvel Ganesan\*, Adam Barowski, Lorenz Ratke, Barbara Milow

Institute of Materials Research, German Aerospace Center, Linder Hoehe, 51170 Cologne, Germany.

Corresponding author email address: k.ganesan@dlr.de

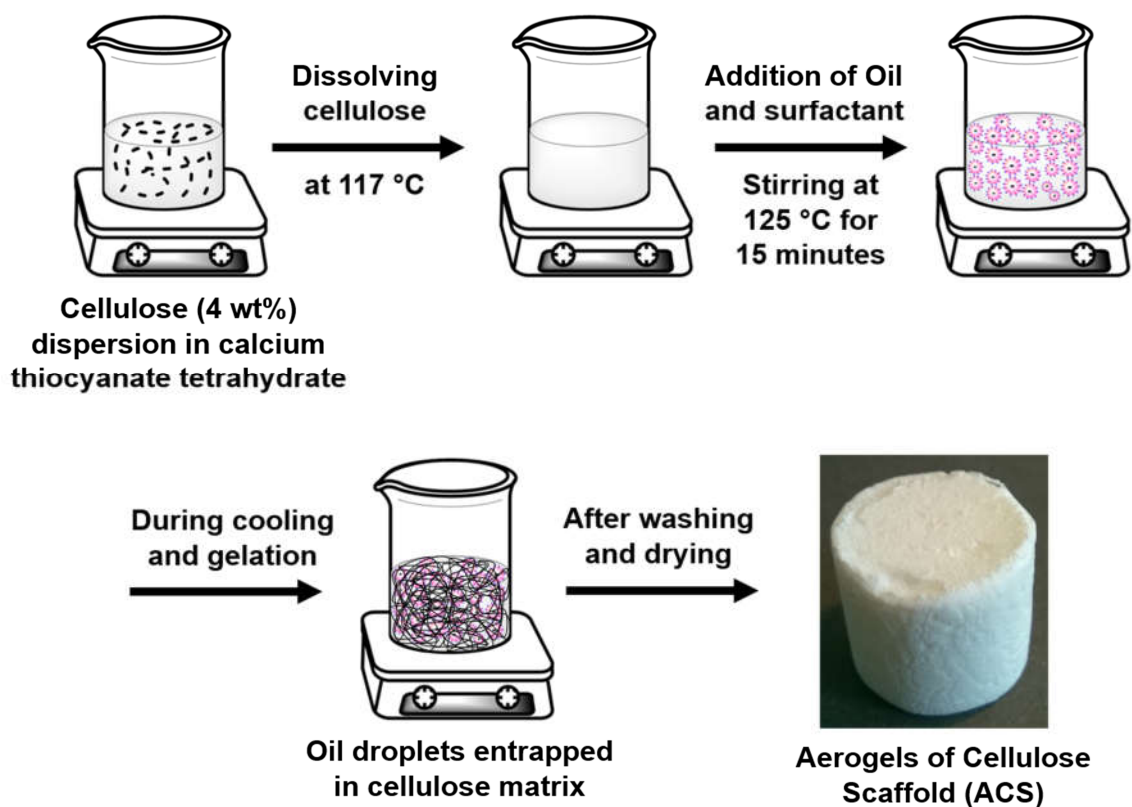


**Figure 1:** Schematic diagram of the method of cellulose scaffolds preparation.

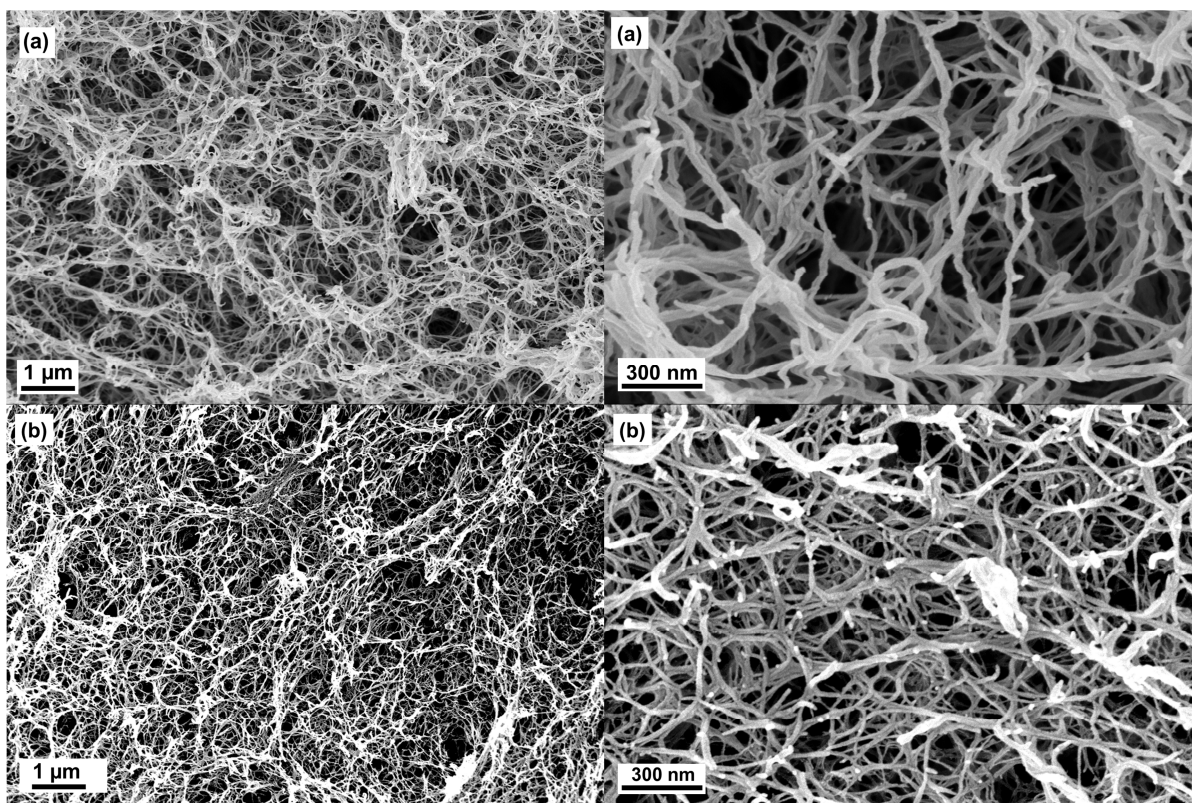


**Figure 2:** Scanning electron microscopy images of classical aerogels of cellulose: (a) AC-2 and (b) AC-4.

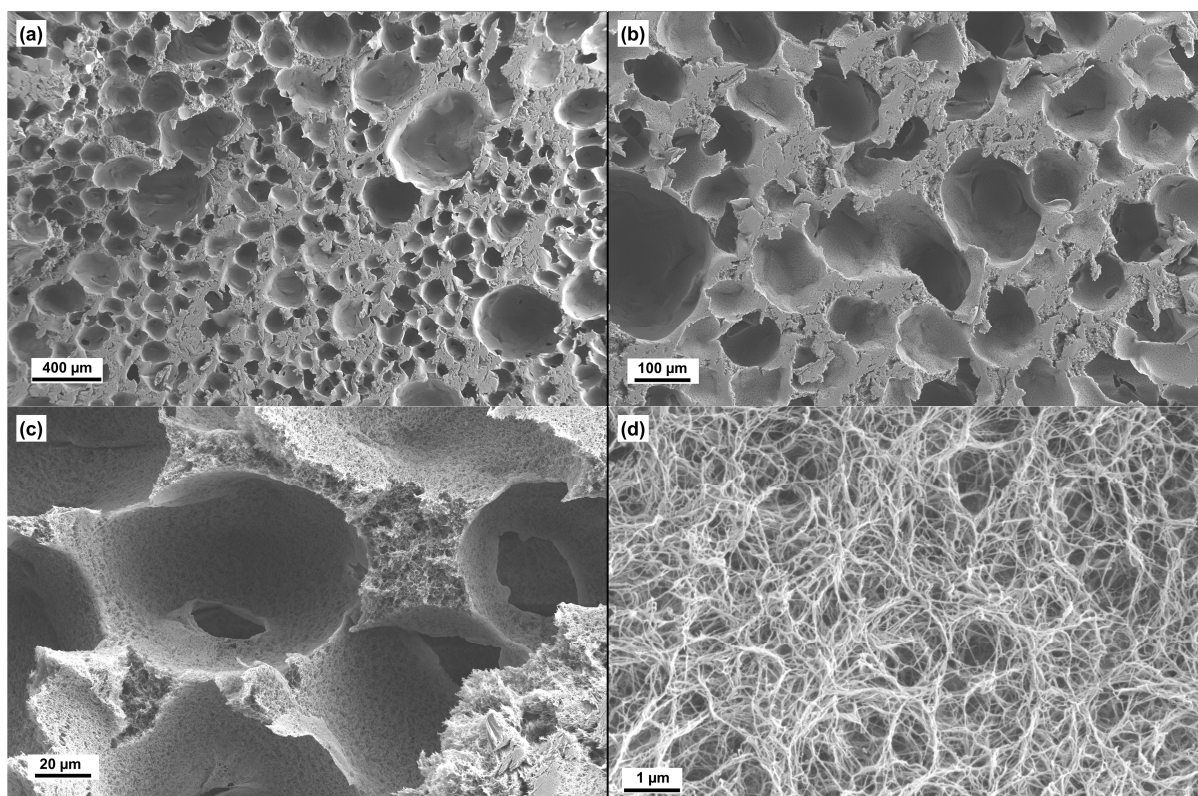


**Figure 3:** Scanning electron microscopy images of aerogels of ACS-PT.

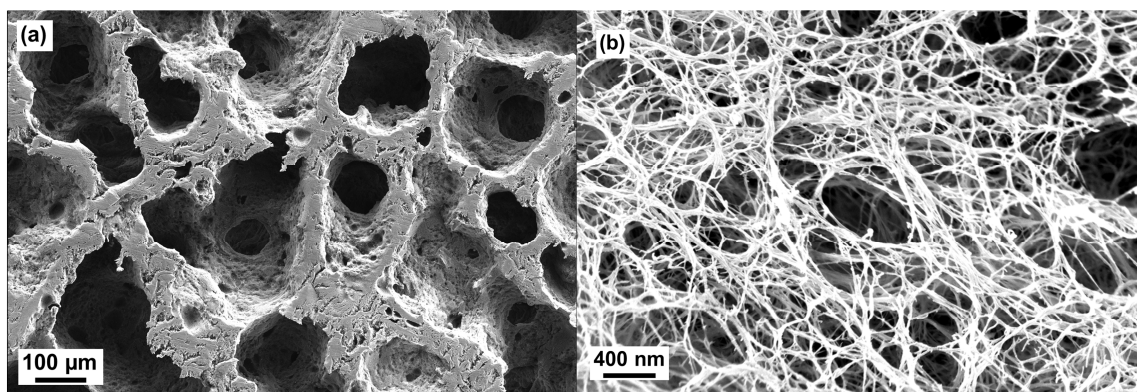


Figure 4: Scanning electron microscopy images of aerogels of cellulose: ACS-PO.

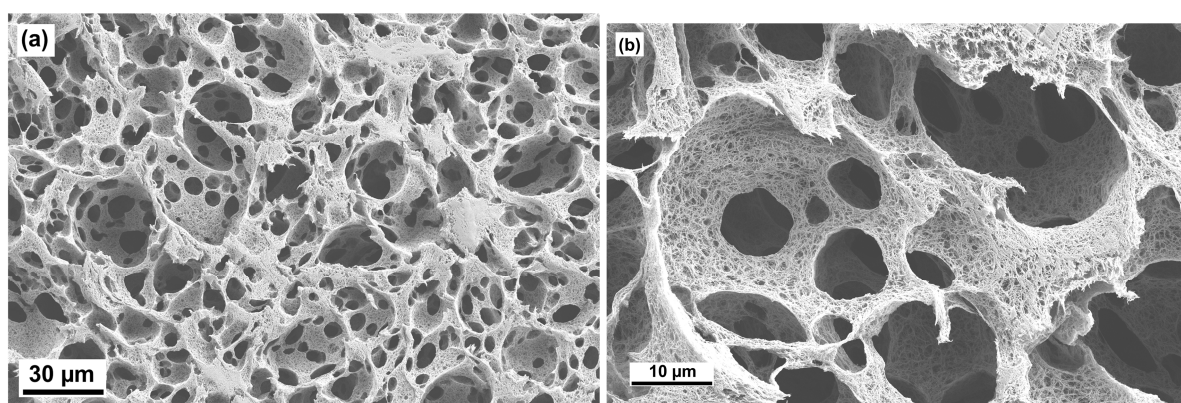
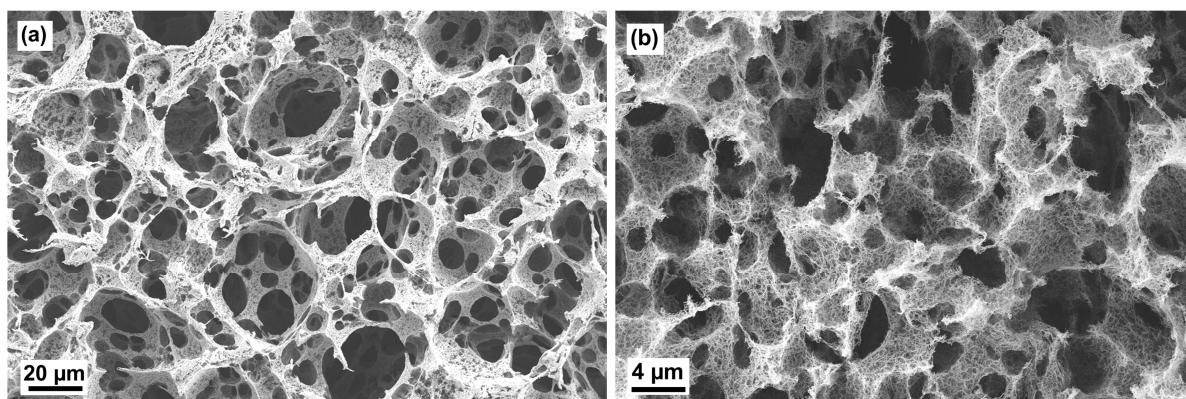
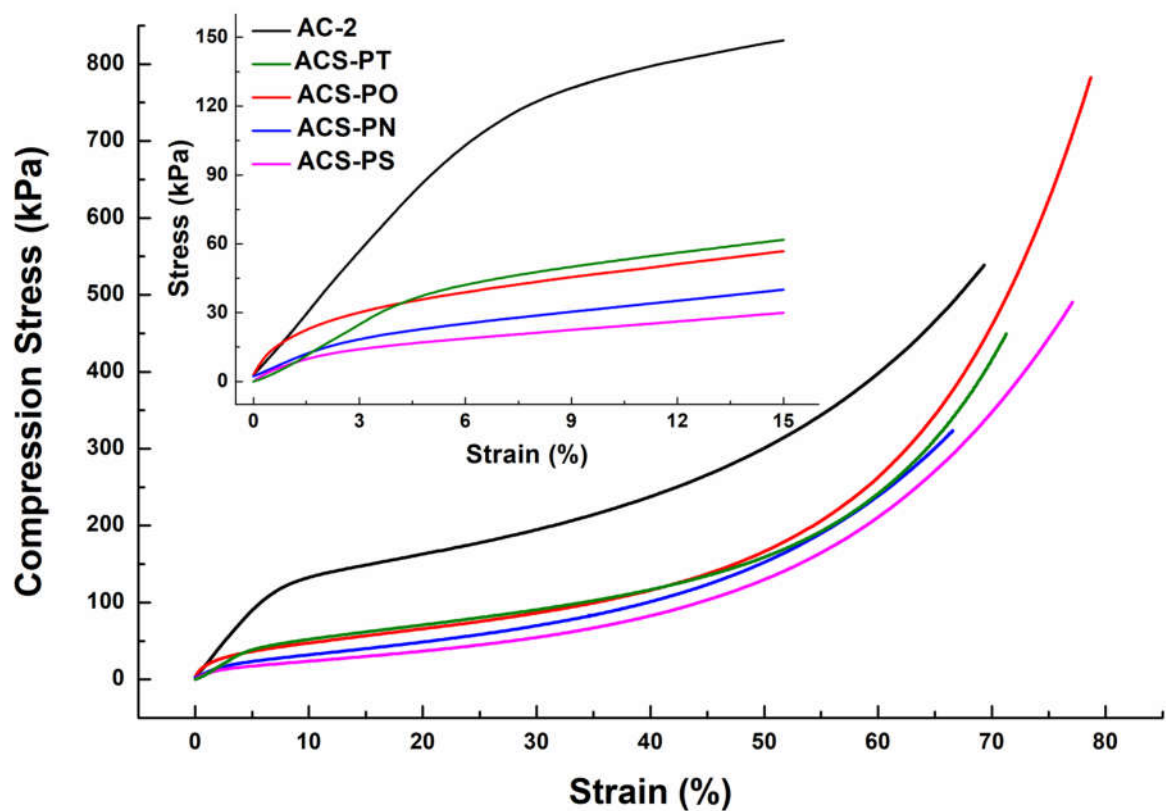


Figure 5: Scanning electron microscopy images of aerogels of cellulose: ACS-PN.



**Figure 6:** Scanning electron microscopy images of aerogels of cellulose: ACS-PS.



**Figure 7:** The compression stress-strain curve of cellulose materials.

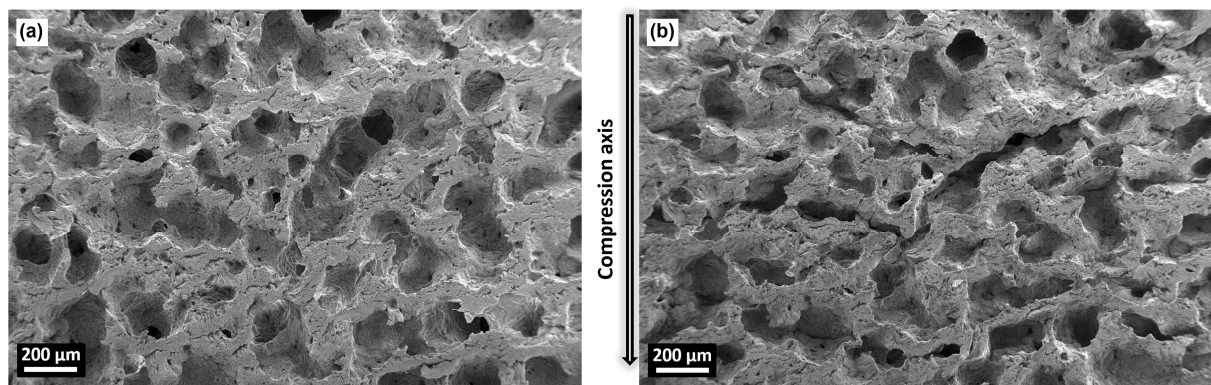


**Figure 8:** Comparison of microstructural changes of ACS-PO: before compression test (a) and after 25 % of compression (b). The compression of the sample occurred from top.

# INFLUENCE OF HIERARCHICAL POROUS STRUCTURES ON THE MECHANICAL PROPERTIES OF CELLULOSE AEROGELS

Kathirvel Ganesan\*, Adam Barowski, Lorenz Ratke, Barbara Milow

Institute of Materials Research, German Aerospace Center, Linder Hoehe, 51170 Cologne, Germany.

Corresponding author email address: k.ganesan@dlr.de

## Supplementary information

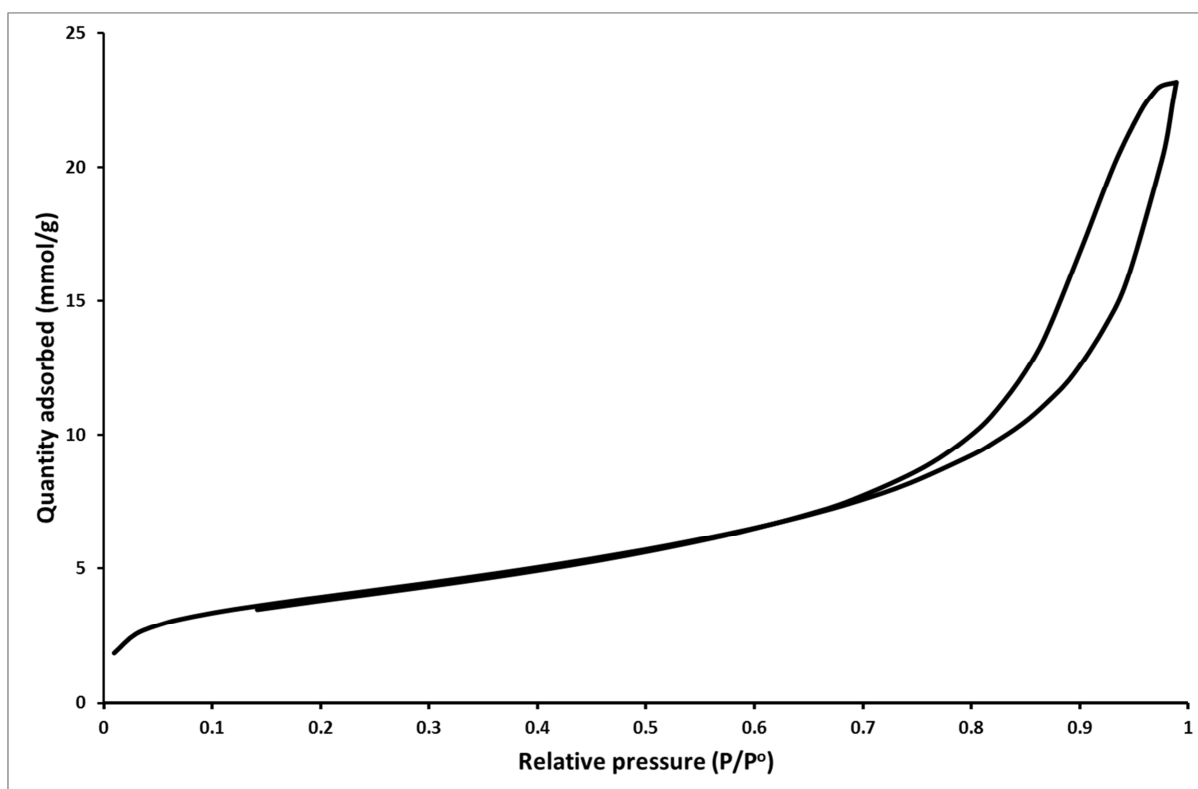


Figure SI-1: Nitrogen adsorption-desorption isotherm linear plot of aerogels of cellulose scaffold (ACS-PT).